CDD*press*

ARTICLE   **OPEN**

Check for updates
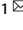
Transglutaminase 2 associated with PI3K and PTEN in a membrane-bound signalosome platform blunts cell death

Károly Jambrovics[1], Pál Botó[1], Attila Pap[1], Zsolt Sarang[1], Zsuzsanna Kolostyák[1], Zsolt Czimmerer[1,2], Istvan Szatmari[1], László Fésüs[1], Iván P. Uray[3] and Zoltán Balajthy [1]✉

Atypically expressed transglutaminase 2 (TG2) has been identified as a poor prognostic factor in a variety of cancers. In this study, we evaluated the contribution of TG2 to the prolonged cell survival of differentiated acute promyelocytic leukaemia (APL) cells in response to the standard treatment with combined retinoic acid (ATRA) and arsenic trioxide (ATO). We report that one advantage of ATRA + ATO treatment compared to ATRA alone diminishes the amount of activated and non-activated CD11b/CD18 and CD11c/CD18 cell surface integrin receptors. These changes suppress ATRA-induced TG2 docking on the cytosolic part of CD18 β2-integrin subunits and reduce cell survival. In addition, TG2 overexpresses and hyperactivates the phosphatidylinositol-3-kinase (PI3K), phospho-AKT S473, and phospho-mTOR S2481 signalling axis. mTORC2 acts as a functional switch between cell survival and death by promoting the full activation of AKT. We show that TG2 presumably triggers the formation of a signalosome platform, hyperactivates downstream mTORC2-AKT signalling, which in turn phosphorylates and inhibits the activity of FOXO3, a key pro-apoptotic transcription factor. In contrast, the absence of TG2 restores basic phospho-mTOR S2481, phospho-AKT S473, PI3K, and PTEN expression and activity, thereby sensitising APL cells to ATO-induced cell death. We conclude, that atypically expressed TG2 may serve as a hub, facilitating signal transduction via signalosome formation by the CD18 subunit with both PI3K hyperactivation and PTEN inactivation through the PI3K-PTEN cycle in ATRA-treated APL cells.

INTRODUCTION

Growing evidence now supports type 2 "tissue" transglutaminase as a fundamental cell survival factor in a number of human cancers, including breast, cervical, colon, lung, and pancreatic cancers, as well as leukaemia and lymphoma [1, 2]. TG2 can function as a signalling protein in its GTP-bound/closed/signalling-active conformations to facilitate the functions of cancer cells, but it can also work as an enzyme in its calcium-bound/open/transamidase-active form. TG2, as a multifunctional protein, shows several non-enzymatic functions that depend on its cellular location, where it plays a variety of roles in physiological and pathophysiological processes [3].

The standard treatment of acute promyelocytic leukaemia (APL), a clinically and biologically distinct variant of AML, includes both targeted transcriptional and differentiation therapy and greatly induces the atypical expression of TG2 in myelocytic cells, such as NB4 cells [4, 5]. Arsenic trioxide (ATO) has also been introduced as an APL treatment, as its addition is associated with extended survival in a large proportion of patients, even when used as a single agent [6, 7]. However, ATO also works in synergy with ATRA to cause degradation of the PML/RARα oncoprotein [8]. Recent studies carried out in front-line treatment have revealed that the ATRA + ATO combination was superior to ATRA and chemotherapy,
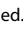
as it substantially reduced the cumulative incidences of relapse while improving disease-free and event-free survival [9, 10].

Using APL as a model, we have addressed the "advantages" of cancer cells expressing TG2 and now propose that the atypical expression of TG2 may alter the signal transduction pathways of these cancer cells. Here, while investigating the cell death process induced by ATO in ATRA-differentiated NB4 cell lines, we found that cell death is attenuated by TG2 expression. We discovered that the plasma membrane-bound form of TG2 functions as a signalling platform that brings CD18, c-SRC, PI3K/p110, PI3K p85, phospho-AKT T308, S473, phospho-mTOR S2481, and S2448 proteins into close proximity, thereby triggering oncogenic hyperactivity of PI3K and robust PTEN inactivation. These platforms are disintegrated into individual components by NC9 (TG2 inhibitor) and by PP2 (c-SRC inhibitor). TG2 therefore may serve as a hub that facilitates signal transduction activation with gain-of-function PI3K and loss-of-function/tumour suppressor PTEN effects in APL.

METHODS

Cell lines

The following APL cell lines were cultured as described previously: NB4 WT (wildtype NB4 cells), NB4 TG2-C (virus control containing scrambled

[1]Department of Biochemistry and Molecular Biology, Faculty of Medicine, University of Debrecen, Egyetem tér 1, Debrecen H-4032, Hungary. [2]Eötvös Loránd Research Network, Biological Research Centre, Institute of Genetics, Szeged, Hungary. [3]Department of Clinical Oncology, Faculty of Medicine, University of Debrecen, Egyetem tér 1, Debrecen H-4032, Hungary. ✉email: balajthy@med.unideb.hu
Edited by Professor Mauro Piacentini

shRNA), TG2-deficient NB4 TG2-KD (shRNA-based knockdown), and NB4 TG2-KO cells (TALEN TG2 knockout) [5, 11, 12].

Gene expression
Methods for the isolation of RNA and RT-PCR/RT-QPCR have been published previously [11, 12].

Annexin-V labelling and sorting of dead NB4 cells
$1-2 \times 10^6$ NB4 treated cells were harvested and labelled with FITC-conjugated Annexin-V (Biolegend) for 15 min according to the manufacturer's instruction. Cells were analysed and sorted on a BD FACSAria III (BD Biosciences, San Jose, CA). Before sorting, first the NB4 cells were gated based on their size and granularity, thereafter the gated and Annexin-V$^+$ cells were sorted.

Western blotting
Preparation of lysate from cell culture and WB analysis have been described previously [11, 12].

Luciferase activity
Luciferase activity was measured using the Bright-Glo™ Luciferase Assay system (Promega) following the manufacturer's instructions.

Transfection of NB4 cells with a FOXO3A lentiviral reporter
A ready-to-transduce transcription factor-responsive lentiviral reporter system (CCS-1022L, QIAGEN) was used to generate a stable cell line, following the manufacturer's protocol. Luciferase activity was measured as previously described [12].

Plasma membrane preparation
The plasma membrane was isolated according to the Abcam protocol (ab65400).

PIP$_3$ extraction and measurement
The isolation of PIP molecules was carried out by chloroform-methanol based organic separation (Supplementary method). Phosphatidyl-inositol levels were determined with an ELISA detection kit (K-2500S, Echelon Biosciences) and normalised to 100 µg protein.

In vivo mouse experiments
NB4 WT and NB4 TG2-KO cells (1×10^7) were washed with sterile phosphate buffered saline (PBS) and injected into the retro-orbital region of 8–9-week-old NOD/SCID (CB17/lcr-Prkdc^{scid}, JANVIER LABS) female mice under sterile conditions. Animals were divided into four groups. Anaesthetised mice were administered vehicle, ATRA at 1.0 mg/kg + DEX at 50 µg, ATO at 0.75 mg/kg or combined ATRA + ATO intraperitoneally every second day for 14 days. A 27.5/0.5-gauge needle/syringe (Terumo U-100, Terumo Medical Corporation, Elkton, MD) was used for the i.p. administration of treatment. DMSO administration was kept under 2% (v/v) to avoid any cytotoxic effects. At the end of the treatment, the mice were anaesthetised with isoflurane for blood sampling. Circulating human and mouse blood cells were analysed from total cardiac blood samples by flow cytometry.

All experiments were performed according to the guidelines of the Institute for Laboratory Animal Research, University of Debrecen, Faculty of Medicine, and were approved by the national and institutional ethics committee for laboratory animals used in experimental research (Project ID:4/2020/DEMAB).

Flow cytometry for human CD11c/CD11b/Annexin-V$^+$ cells
To assess the survival of human NB4 cells in mice, blood was collected and red blood cells were lysed in lysis buffer (BD PHarmn Lyse™), thereafter mouse macrophages were stained with F4/80-APC antibody (1:100x; Biolegend) for 15 min in the dark at 4 °C. F4/80$^-$ cells were sorted and labelled with CD11c-PE and CD11b-FITC antibodies (1:25; R&D Systems) and APC-conjugated Annexin-V (Biolegend) for 15 min at 4 °C in the dark, and then analysed with a BD FACSAria III flow cytometer. The FACS data were analysed with Flowing 2.0.5 and normalised/corrected with isotype controls.

Immunoprecipitation (IP)
IP was performed following the Thermo Fisher protocol (Supplementary methods). The isolated plasma membrane fractions were analysed by LC-MS/MS by the Proteomics Core Facility, Faculty of Medicine, University of Debrecen.

Statistical analysis
Statistical analyses were carried out using GraphPad Prism 8.0.9 with Student's t test and two-way ANOVA ($*P < 0.05$, $**P < 0.01$, $***P < 0.001$).

RESULTS

Transglutaminase 2 lowers ATO-induced cell death in ATRA-differentiated NB4 cells
NB4 cell lines were differentiated with ATRA with or without ATO at 0.5 or 2.0 µM. Differentiation with ATRA alone stopped cell proliferation after two days in all cell lines (Fig. 1A); however, the addition of ATO decreased the cell counts in a dose-dependent manner (Fig. 1B).

Annexin V-positivity in response to ATRA or ATO, determined by Flow cytometry analysis during the five-day period, showed that ATRA induced a minor degree of cell death (Fig. 1B), while TG2 induction [12] by the ATRA + ATO (0.5 or 2.0 µM) treatment was associated with lower cell death rates in NB4 WT compared to NB4 TG2-KO cells, suggesting that cell survival was TG2-dependent. The complete elimination of TG2 (NB4 TG2-KO) increased the susceptibility to cell death induced by ATRA + ATO treatment compared to the NB4 TG2-WT (Fig. 1B day 3–5). ATO (0.5 or 2.0 µM) treatment alone caused similar changes in cell numbers to ATRA + ATO (0.5 or 2.0 µM) treatment and the extent of induction of cell death is shown (Supplementary Fig. 1A, B). Overall, these data indicated that TG2 expression associated with ATRA-induced differentiation contributed to cell survival.

ATO suppresses the ATRA-induced expression of leucocyte β2-integrin receptors CD11b/CD18 and CD11c/CD18
ATRA treatment enhances the expression of CD11b/CD18 and CD11c/CD18 integrin receptors, while also activating them to a high-affinity (extended-open) form [12]. ATO treatment significantly influences the rate of cell division and induces apoptosis. We therefore examined mRNA expression of both receptors following ATRA and ATO treatments at day 0, 3, and 5. CD11b mRNA expression showed a time-dependent, but TG2-independent pattern, increased during ATRA treatment, whereas ATO treatment limited this expression (Fig. 2A). ATO treatment alone induced a low and time-dependent mRNA expression (Supplementary Fig. 2A–C). In contrast, no major differences were noted in the levels of non-active (bent-closed) CD11b/CD18 cell surface receptors in response to 0.5 or 2.0 µM ATO. However, on the fifth day, the expression of CD11b/CD18 receptors decreased following the combined treatments (Supplementary Fig. 2). The amounts of activated cell surface CD11b/CD18 receptors with a high-affinity state also increased continuously with the combined treatment but remained significantly lower than in cells treated with ATRA alone (Fig. 2B).

CD11c mRNA expression was barely induced by single ATO treatments in NB4 cell lines (Supplementary Fig. 2G–I). In contrast, the CD11c mRNA levels increased robustly and, in a time-dependent manner with ATRA treatment, but this increase was mitigated in a concentration-dependent manner by the addition of ATO (Fig. 2C). Comparison of the expression of non-active CD11c/CD18 (bent-closed) cell surface receptors revealed that the addition of ATO blunted the ATRA-induced CD11c/CD18 expression (Supplementary Fig. 2P–R). The use of an antibody (Clone 3.9) that detected the activated (extended-open) form of cell surface CD11c/CD18 revealed a similar response to ATRA and ATO treatments to that seen for mRNA (Fig. 2D). Thus, these data
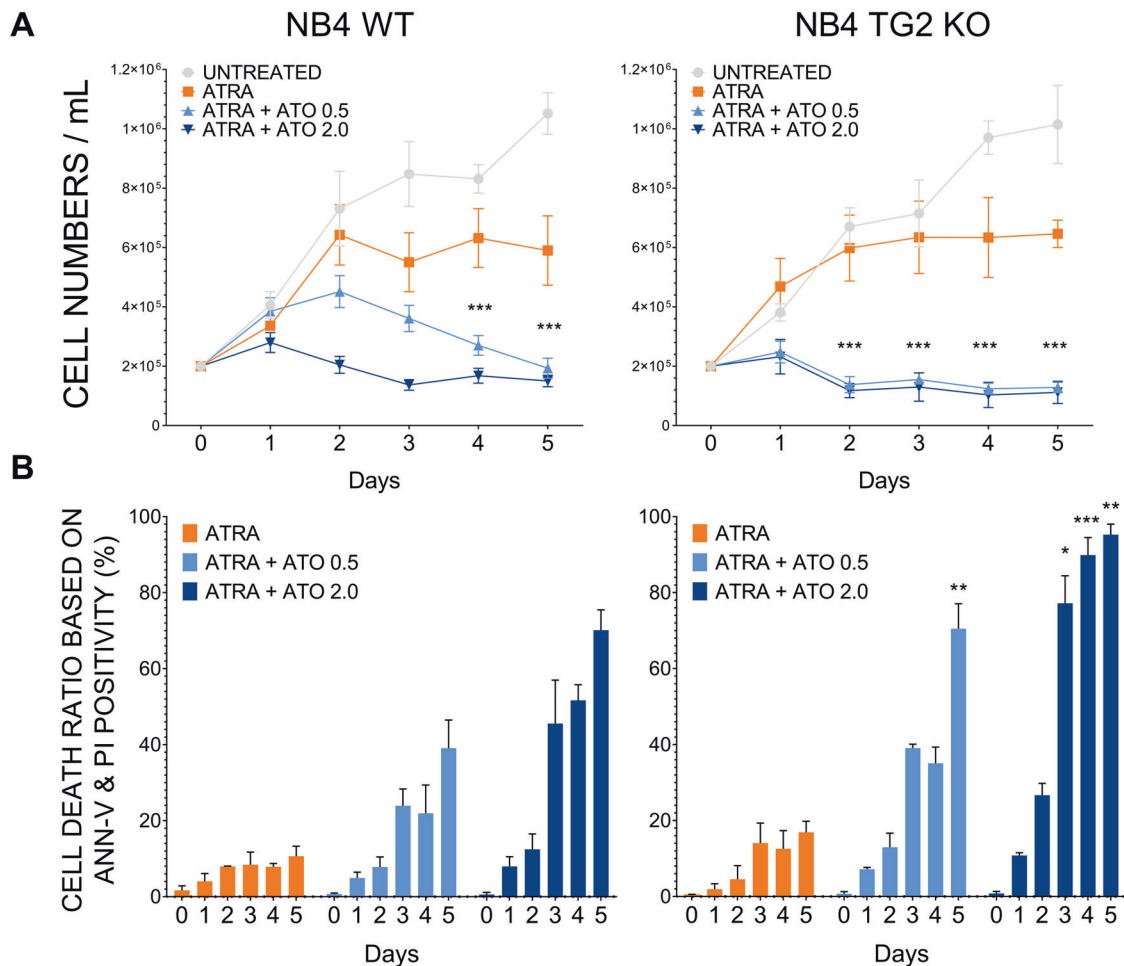
Fig. 1 Transglutaminase 2 lowers ATO-induced cell death. A Cell number changes measured in KOVA Glasstic® Slide cell number counting chambers following treatment of NB4 WT and NB4 TG2-KO cells without treatment (UNTREATED) or with 1 μM ATRA; 1 μM ATRA + 0.5 μM ATO; and 1 μM ATRA + 2.0 μM ATO at the indicated days ($n = 13$). Asterisk are representing the significant differences between the ATRA – ATO treatment versus ATRA treatment. **B** FACS analysis of Annexin-V and PI stained NB4 cell lines following ATRA or ATRA + ATO treatment. The percentage of cell death ratio is represented as mean % ±SD ($n = 9$). Measurements were conducted in triplicates; values were validated by Flowing software 2.5.1. Statistical analysis was conducted by two-way ANOVA (Bonferroni post-hoc test; *$p < 0.05$, **$p < 0.01$ and ***$p < 0.001$, ****$p < 0.0001$). Asterisk show the significant differences in NB4 WT vs. NB4 TG2-KO cell lines.

indicate that the activated and non-activated forms of CD11b/CD18 and CD11c/CD18 receptors remained significantly lower with the combined treatment than in cells treated with ATRA alone.

ATRA-induced TG2 boosts the phosphorylation of mTORC2 and keeps FOXO3 transcriptionally inactive

The PI3K, AKT/Protein Kinase B, and mTOR signalling pathways are critical for the regulation of cell growth and survival. mTORC1 is phosphorylated mainly on Ser2448 of mTOR, whereas mTORC2 is mainly phosphorylated on Ser2481 of mTOR [13, 14]. ATRA-differentiated NB4 cells showed phospho-S2481-mTOR levels that changed with the amount of TG2. The appearance of phospho-S2481-mTORC was significantly higher in differentiated NB4 WT and virus control NB4 TG2-C cells than in NB4 TG2-KD or TG2-deficient NB4 TG2-KO cells, and it was also associated with the decreased phosphorylation of AKT at Ser473 (Fig. 3A–D; first block). The degree of phosphorylation of mTORC-S2448 did not correlate with TG2 expression (Fig. 3A, first block).

PIP$_3$ activates PDK1 to trigger the phosphorylation of AKT at Thr308 [15]. Although AKT Thr308 phosphorylation appeared to be TG2-independent, the 473-Serine side chain was phosphorylated to a significantly greater extent at ATRA-induced TG2 protein levels (in NB4 WT and NB4 TG2-C cells) than when TG2 expression

was low or absent (in NB4 TG2-KD and NB4 TG-KO cells) (Fig. 3C, D, first block). The combination of ATRA with either 0.5 or 2.0 μM ATO had the same effect on the amount of phospho-S2481-mTOR as ATRA alone (Fig. 3A, B, second and third blocks). By contrast, a concentration-dependent suppression of AKT Ser473 phosphorylation occurred after ATO treatments and was independent of the levels of S2481-phosphorylation of mTOR (Fig. 3C, D, second and third blocks, Supplementary Fig. 3A).

FoxO transcription factors are major downstream targets of the PI3K-AKT signalling pathway controlling cell proliferation and survival. Phosphorylation by AKT results in the nuclear export and cytoplasmic sequestration of FOXO, thereby inhibiting its transcriptional activity and promoting cell survival, growth, and proliferation [16–18]. In ATRA-treated cells, phosphorylated-FOXO3 amounts increased gradually relative to total FOXO3 expression until day 5 (Fig. 3E, first block). In contrast, ATRA + ATO treatment attenuated and delayed the induction of phosphorylated FOXO3, while significantly increasing the total amount of FOXO3 protein (Fig. 3E, second and third blocks). In the absence of TG2, the phosphorylated FOXO3 levels were practically unchanged in ATRA-treated NB4 TG2-KO cells up to day 5, whereas the total FOXO3 protein levels increased slightly from day 3 to day 5, ATRA + ATO treatment intensified that (Fig. 3F, H).
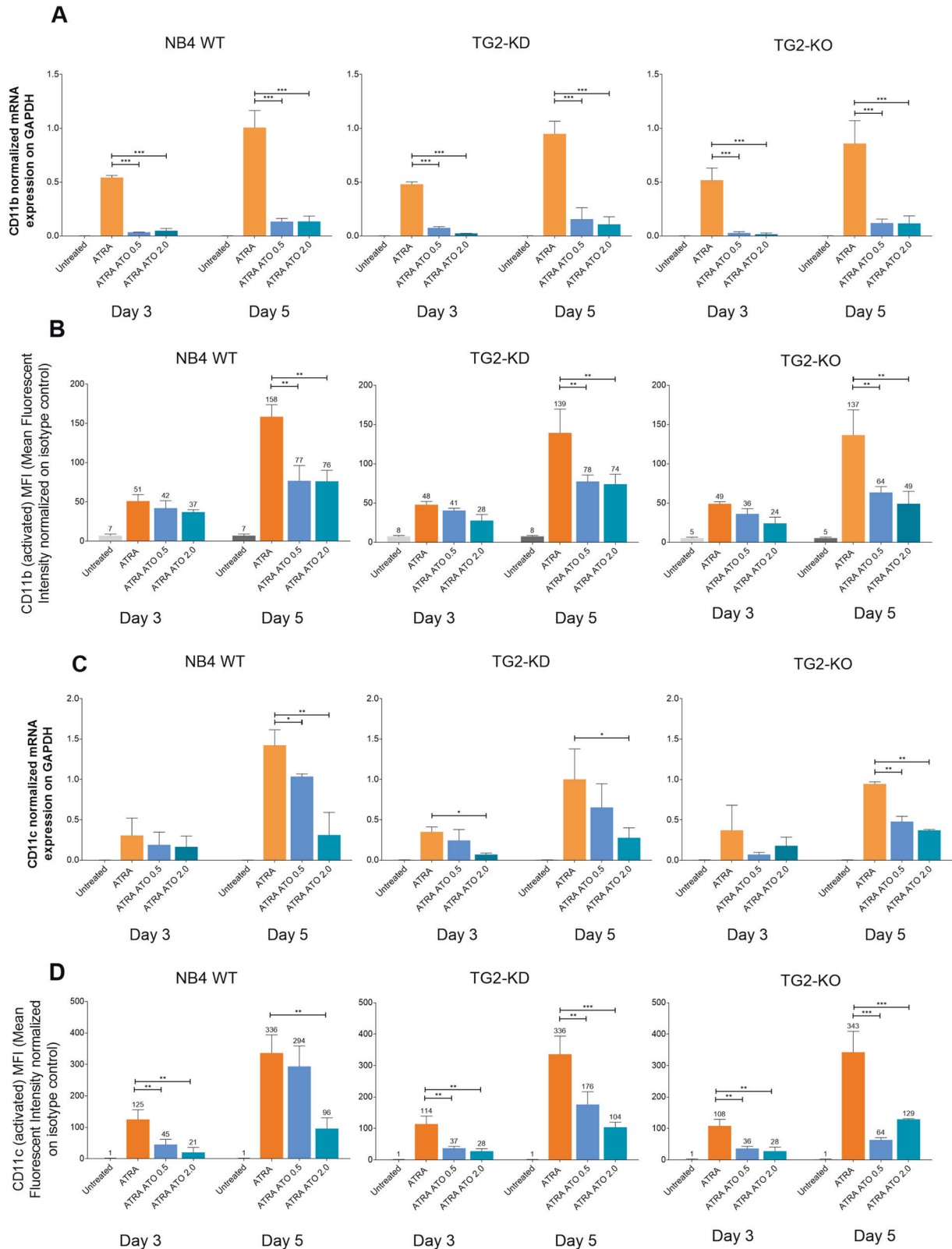
Fig. 2 ATO suppresses the expression of leucocyte β2 integrin CD11b/CD18 and CD11c/CD18. A Relative mRNA expression of CD11b at the indicated days by RT-qPCR normalised to GAPDH ($n = 3$). **B** Flow cytometry analysis of cell surface expression of the differentiation marker CD11b/CD18 ($n = 3$). **C** Relative mRNA expression of CD11c measured by RT-qPCR normalised to GAPDH ($n = 3$). **D** Flow cytometry analysis of cell surface expression of differentiation marker CD11c/CD18 ($n = 3$). Measurements were conducted in triplicate; values were validated by Flowing software 2.5.1. Statistical analysis was conducted by two-way ANOVA (Bonferroni post hoc test; *$p < 0.05$, **$p < 0.01$ and ***$p < 0.001$, ****$p < 0.0001$).
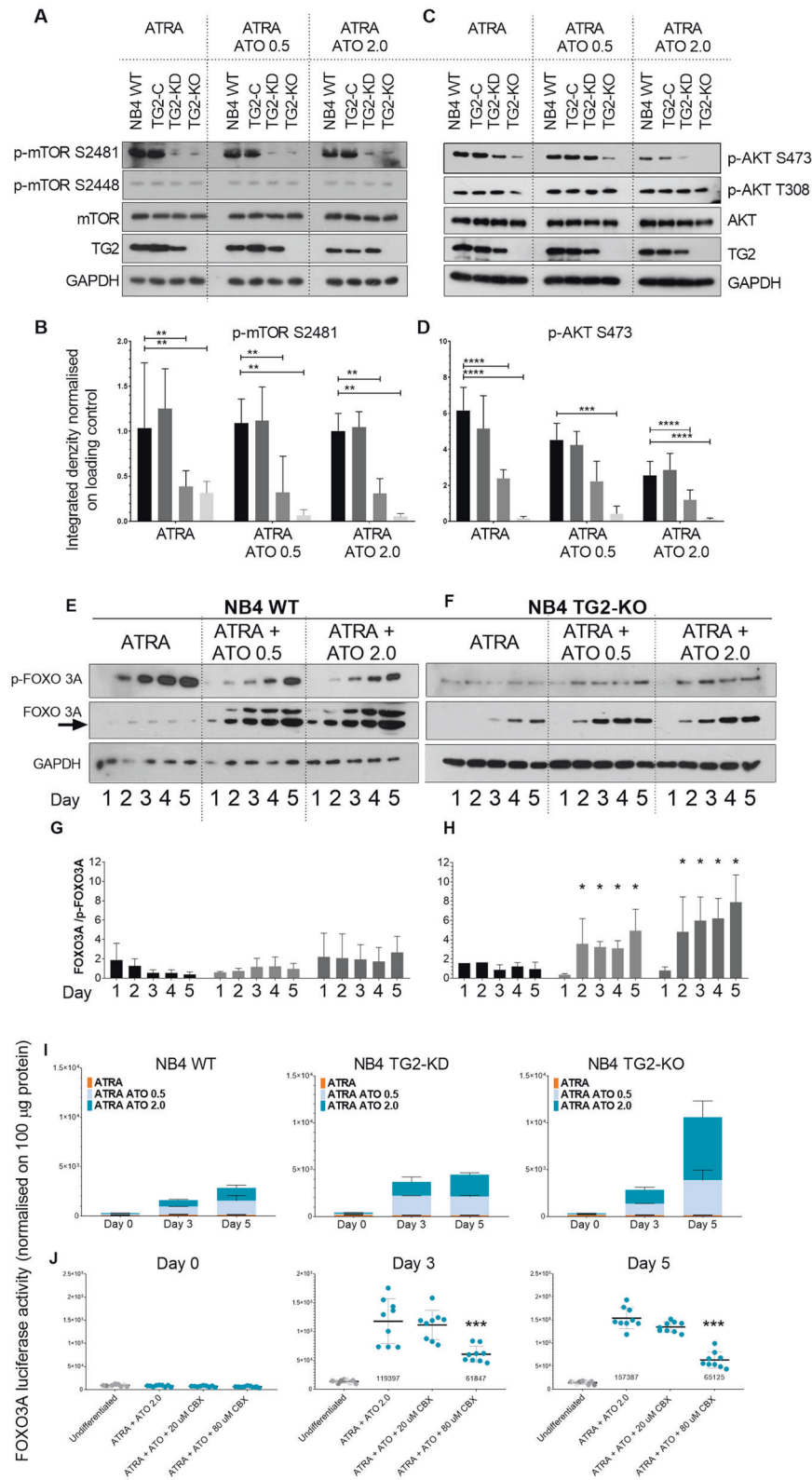
The examination of FOXO3 transcriptional activity using the FOXO3A response element driven luciferase construct stably integrated into the NB4 cell genome revealed that increasing ATO concentrations were associated with enhanced luciferase reporter activity in cells expressing no or low TG2 levels (Fig. 3I). TG2 expression inhibited the transcriptional activity of FOXO3 (Fig. 3I,

first column) via the AKT S473 phosphorylated form (Fig. 3C, D, first block). In the presence of ATO and the absence of TG2, AKT S473 remained unphosphorylated (Fig. 3C, D, third blocks) and was associated with a significant increase in FOXO3 transcriptional activity (Fig. 3I, third column). Treatment with Carbenoxolone (CBX), a potential FOXO3 inhibitor, reduced the luciferase reporter

6

Fig. 3 TG2 boosts the phosphorylation of mTORC2 and maintains FOXO3 transcriptionally inactive. A, C Representative western blot showing p-mTOR (2481, 2448) p-AKT (S473, T308), mTOR, AKT, TG2, and GAPDH protein expression levels in NB4 cell lines after 5 days ($n = 9$). **B, D** Densitometry analysis results represent integrated optical density normalised to a loading control. **E, F** Representative western blot showing p-FOXO1/FOXO3/FOXO4 (T24/T32), FOXO3A and GAPDH protein expression levels for 5 days ($n = 5$). **G, H** Densitometric analysis of the FOXO3A and phosphorylated FOXO3A blots. **I** NB4 cell lines containing a FOXO3A luciferase reporter element were treated and measured by a luminescence-based method in triplicate and reported as relative light units (RLU) ($n = 3$). Values are normalised to 100 μg cell lysate protein from each cell line. **J** NB4 cell lines containing the FOXO3A luciferase reporter element were treated with ATRA or ATRA + ATO with or without the FOXO3A inhibitor CBX and measured by the luminescence-based method in triplicate and reported as RLU. Values are normalised to 100 μg cell lysate protein from each cell line. Statistical analysis was conducted by two-way ANOVA (Bonferroni post hoc test; $*P < 0.05$, $**P < 0.01$ and $***P < 0.001$, $****P < 0.0001$).

activity driven by the FOXO3A promoter by 48.2% at day 3 and 58.7% at day 5 in ATRA + ATO treated NB4 WT cells (Fig. 3J). Annexin-V positivity decreased by 13% and 9% at days 3 and 5, respectively, in parallel with the reduced FOXO3A transcriptional activity (Supplementary Fig. 3B–F). Collectively, these data indicate a potential role of TG2 to increase phosphorylation of mTOR on Ser2481 suppressing transcriptional activity of FOXO3A.

TG2 is required for enhanced PI3K-AKT-TOR signal transduction pathway activity

Our working hypothesis was that atypical TG2 expression sustains cell survival by activating the mTORC2, Phospho-AKT (S473, T308), and Phospho-FOXO3 signalling pathways. The binding of growth factors to a RTK can activate PI3K to generate PIP_3 whose concentration has been determined in NB4 cell lines. The PIP_3 results confirmed that ATRA treatment of NB4 WT cells increased the PIP_3 level by about 180,000-fold compared to NB4 TG2-KO cells. The PIP_3 levels were 11,000 times higher in NB4 TG2-KD cells than they were in TG2-KO cells (Fig. 4A), and the ATRA + ATO treatment, with the exception of the ATRA + ATO treatment seen in Fig. 4B, had no effect on this trend. The PIP_3 content of undifferentiated dividing NB4 cell lines was about one-tenth that of differentiated non-dividing NB4 WT cells (Supplementary Fig. 4). Sorting of the ATRA- and ATRA + ATO-treated NB4 cell lines for live and apoptotic cells revealed PIP_3 concentrations that were 7-fold higher in Annexin-V negative NB4 WT cells and 2-fold higher in TG2-KD cells than in NB4 TG2-KO cells (Fig. 4C). The PIP_3 levels were significantly lower in apoptotic Annexin-V-positive cells of every cell line compared to live cells (Fig. 4D).

The efflux of PIP_3 is determined by the amounts of monomeric PI3K/p110, PTEN, and phospho-PTEN (Fig. 4E). The expression of PI3K/p110, the PI3K-p85 regulatory subunit, and phospho-PI3K p85 showed TG2 dependency (Fig. 4F–H, first four columns). High TG2 expression was accompanied by increased amounts of PI3K/p110 (Fig. 4F), phospho-PI3K p85 (Fig. 4G), PI3K p85 (Fig. 4H), and phospho-PTEN (Fig. 4I), whereas low (TG2-KD) or no (TG2-KO) TG2 expression was associated with levels one-third and one-fifth of WT, respectively. The phosphatase-active PTEN expression showed a moderate inverse correlation with TG2 expression (Fig. 4J, first four columns), whereas the phosphatase-inactive p-PTEN displayed a powerful proportional correlation with TG2 (Fig. 4I, first four columns). Phosphatase-inactive phospho-PTEN patterns also correlated with patterns of PI3K/p110 and phospho-PI3K p85 expression, suggesting that TG2 induction may support PIP_3 synthesis (Fig. 4F, G, I, first two columns), whereas low TG2 expression was associated with minimal PIP_3 synthesis (Fig. 4F, G, I; third and fourth columns). In WT cells, ATRA + ATO treatment moderately decreased the amount of phosphatase-inactive phospho-PTEN (Fig. 4I, right block), whereas phosphatase-active PTEN was increased in TG2-KD and KO cells (Fig. 4J, right block). PI3K, PI3K p85 and PTEN mRNA expressions were strongly correlated with the Western-blot results shown in Fig. 4K–M. The levels of PI3K-p110 mRNA, PI3K-p85 mRNA, and PTEN mRNA (Fig. 4K–M) showed apparent TG2 dependence. Together, our data show that, while apoptotic cells contain virtually no PIP_3,

differentiated NB4 WT cells expressing TG2 possess ten times more PIP_3 than dividing undifferentiated cells expressing no TG2.

TG2 sustains cell survival by forming a signalosome platform and hyperactivating the PI3K p-AKT S473 and p-mTORC2 signalling axis

The in vivo requirement for TG2 for the survival of NB4 cells was examined by the intravenous injection of 1×10^7 NB4 WT and TG2-KO cells via the suborbital vein into NOD/SCID mice [19]. After 14 days, FACS and Alu-based real-time PCR methods confirmed that blood samples from control, ATRA and ATO treated mice, respectively, contained comparable numbers of NB4 WT and TG2-KO cells (NB4 WT 4681740 vs TG2-KO 4100983) [11, 19]. Only the ATRA + ATO treatment reduced the NB4 TG2-KO cell counts below WT levels (Fig. 5A).

The antiapoptotic effect of TG2 was then investigated by sorting the ATRA + ATO-treated NB4 cells by Annexin-V staining and analysing them by Western blotting for the expression of TG2, AKT, phospho-AKT (S473, T308), mTOR, phospho-mTOR (S2448, S2481), and procaspase-3 and its truncated forms (Fig. 5B). The immunoblotting results showed reduced amounts of AKT S473 phosphorylation at low TG2 expression, with both being undetectable in TG2-KO cells. Phospho-mTOR S2481 expression also showed TG2 dependence. Apoptotic markers, in the form of cleaved caspase 3 and procaspase-3, were present in higher amounts in cells with lower TG2 expression (e.g., NB4 TG2-KD or TG2-KO cells) (Fig. 5B, left block). Significant amounts of TG2 were detected in the living Annexin-V-negative WT NB4 and TG2-C cells, but not in the TG2-KD cells. The phosphorylation of AKT S473 and mTOR 2481 decreased in proportion to the amount of TG2. Procaspase-3 and its cleaved forms were below the detection limit (Fig. 5B, middle panel).

In Annexin-V-positive, apoptotic NB4 WT, TG2-C, and TG2-KD cells, no TG2 was detected, and AKT T308 phosphorylation was reduced in all cell lines. However, the loss of TG2 in dying cells was associated with the suppression of phospho-AKT S473 and phospho-mTOR S2481 levels. The levels of procaspase-3 and its cleavage forms were clearly higher than in the unsorted cell populations (Fig. 5B, right panel).

The synthesis of PIP_3 was localised to the cell membrane and appeared to depend on TG2 (Fig. 4A–M), prompting the question of how TG2, which is commonly considered a cytoplasmic protein, might form an association with the plasma membrane. Mass spectrometry analysis of the plasma membrane fraction of NB4 cells identified several hundred proteins. Of these, the CD18 integrin protein was pulled down in a complex that was immunoprecipitated with a TG2 antibody. TG2 also co-immunoprecipitated with CD18; therefore, we concluded that CD18 forms plasma membrane-associated protein complexes with TG2 in differentiated NB4 cells (Fig. 5C). TG2 was detected in a membrane-associated form, leading us to suspect that TG2 might cooperate with proteins, such as c-SRC, PI3K/110, PTEN, and mTOR, that lie downstream in the PI3K-AKT-mTOR signal transduction cascade and participate in protein-protein interactions. Co-immunoprecipitation experiments with the polyclonal TG2 antibody detected interactions between the TG2, CD18,
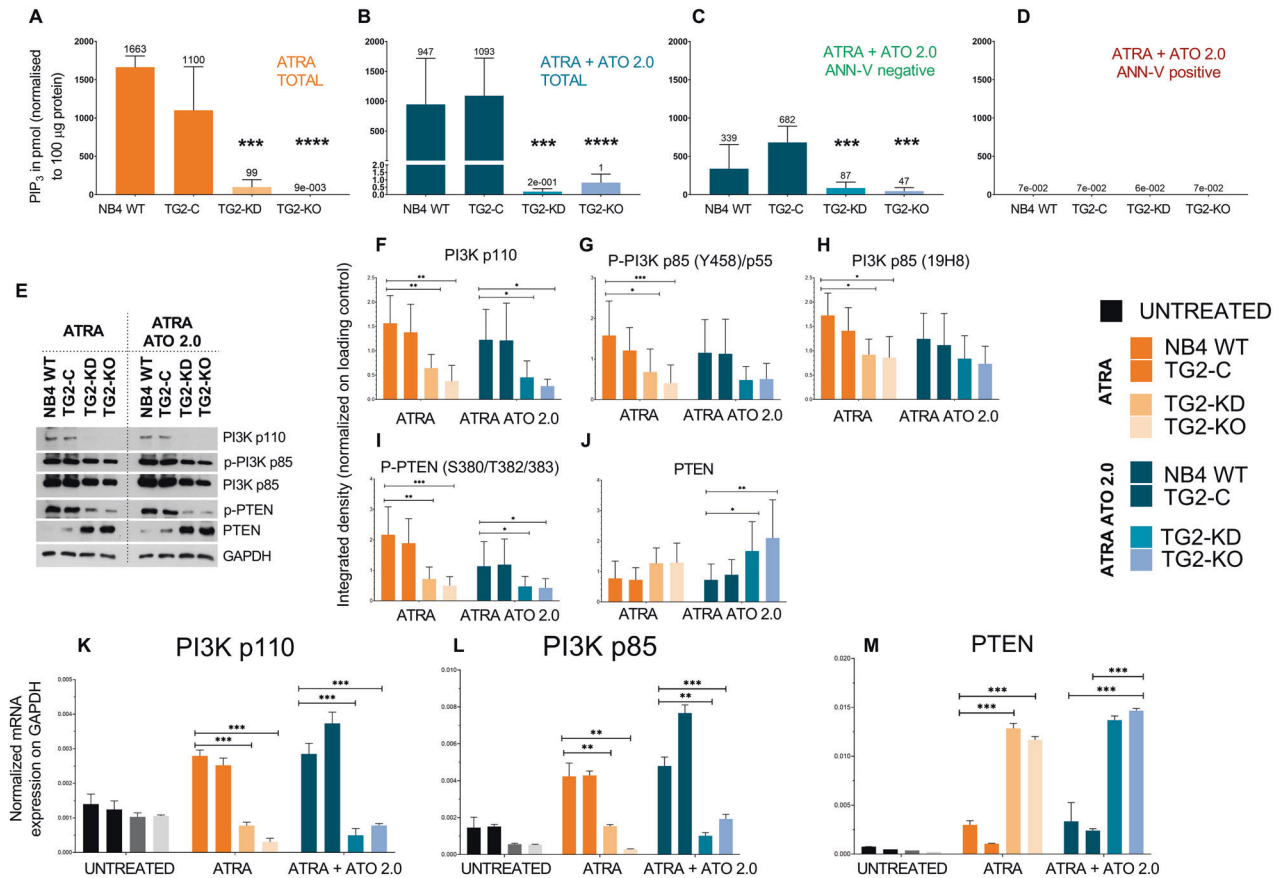
Fig. 4 TG2 is required for enhanced PI3K-AKT-mTOR signal transduction pathway activity. A–D Membrane PIP_3 levels were quantified by an ELISA-based fluorescence detection method (Echelon Inc.). Figures show the representation of the mean values ±SD of PIP_3 levels from three independent experiments ($n = 3$). Measurements were conducted in triplicate. **A** PIP_3 levels in ATRA-treated total NB4 cells. **B** PIP_3 levels in ATRA + ATO treated unsorted NB4 cells. **C** PIP_3 levels in ATRA + ATO-treated Annexin-V labelled but Annexin-V negative cells. **D** PIP_3 levels in ATRA + ATO-treated Annexin-V labelled and Annexin-V positive cells ($n = 3$). **E** Representative western blot showing PI3K subunits, p-PTEN, PTEN, and GAPDH protein expression levels in NB4 cells treated for 5 days with ATRA or ATRA + ATO ($n = 5$). **F–J** Densitometry analysis of western blots of PI3K pathway proteins. **K–M** Relative mRNA expression of *PI3K-p110, PI3K-p85,* and *PTEN* in NB4 cells treated with 1 μM ATRA or 1 μM ATRA + ATO; RT-qPCR results are normalised to GAPDH ($n = 3$). Statistical analysis was conducted by two-way ANOVA (Bonferroni post hoc test; $*p < 0.05$, $**p < 0.01$ and $***p < 0.001$, $****p < 0.0001$).

c-SRC, phosphorylated mTOR (S2481, S2448) from mTORC1 and mTORC2, phospho-AKT (S473, T308), PI3K/p110 and PI3K phospho-p85 (Fig. 5D, 1st and 2nd vertical panel). At the same time, antibodies to mTOR, AKT, CD18, p85, PI3K/p110, PTEN, and c-SRC also co-immunoprecipitated with TG2 in the reciprocal co-immunoprecipitation experiments (Fig. 5D, 1st and 2nd horizontal panel). Treatment for 5 days with either the NC9, TG2 inhibitor or the PP2, c-SRC inhibitor abolished all interactions between TG2 and its interacting proteins.

As the reciprocal co-immunoprecipitation revealed the interacting binding partners of cell membrane-localised TG2, we applied a modified far-western blot analysis using disuccinimidyl suberate (DSS) to stabilise the protein-protein interaction on the membrane in situ [20–22]. Bait proteins (TG2, mTOR, AKT, p85, p110, CD18, PTEN, SRC) were co-immunoprecipitated from plasma membrane, renatured and incubated with plasma membrane lysates. The bound pray proteins were detected by a primary antibody to identify the position of the bait proteins (Fig. 5F). We used the same experimental approach and found that after two days of differentiation, only the rudimentary requirements for the creation of the signalosome were present in NB4 WT cells, suggesting that the assembly of the signalosome is a time-dependent process (Supplementary Fig. 6). Finally, far-western blot analysis with CD18$^{-/-}$ cells showed that TG2 bound to all co-immunoprecipitated proteins except CD18 and SRC (Fig. 5G) and

CD18 antibody could not detect the TG2 and SRC bait proteins as seen on the fourth blot of the second-row of Fig. 5F. These experiments demonstrate that TG2 could support cell survival in vivo based on the formerly unknown capability of TG2 to form signalosome platforms by interacting with CD18.

DISCUSSION
The normal front-line therapy for APL has been the simultaneous administration of ATRA and chemotherapy. However, clinical studies have now revealed that ATO, either alone or in combination with ATRA, can improve the outcomes of APL. Here, we showed that the survival of APL leukaemic cells depends on an active PI3K-AKT-mTORC pathway and a transcriptionally inactive FOXO3 signalling axis TG2 dependent manner in the combined treatments.

TG2 is known to modulate gene expression, and our findings show that it can reciprocally regulate *PI3K* and *PTEN*. However, the differences in enzyme activities in the presence or absence of TG2 expression does not explain the nearly 180,000-fold difference in PIP_3 levels, suggesting that TG2 also enhances PIP_3 production through some other mechanism that does not involve gene expression differences. PIP_3 is present in minute amounts in the membranes of apoptotic cells (Fig. 4D), suggesting that the PI3K-AKT survival signalling pathway is inactivated in dying cells, whereas live Annexin-V negative cells contain high PIP_3 levels (Fig.
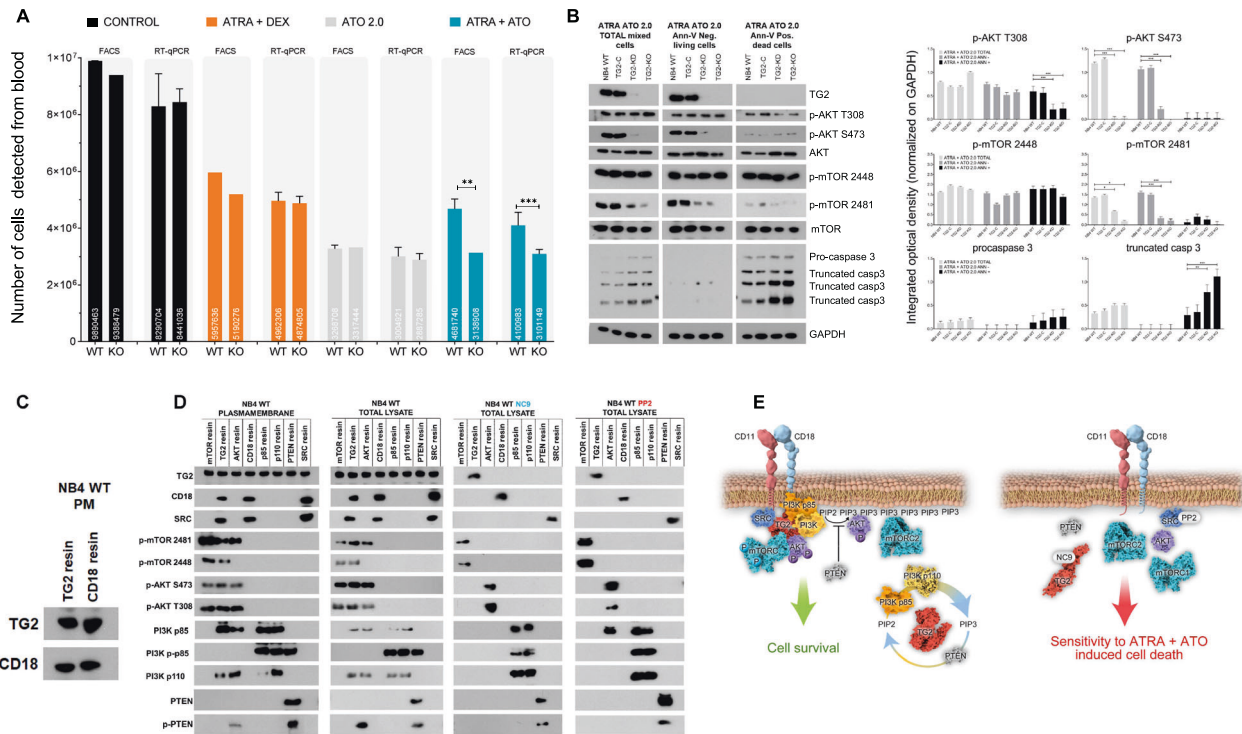
Fig. 5 TG2 sustains cell survival by forming a signalosome platform and hyperactivating the PI3K p-AKT S473 and p-mTORC2 signalling axes. A NB4 WT and TG2-KO cells (1×10^7) were intravenously injected via the suborbital vein into NOD/SCID female mice, followed by intraperitoneal injection of ATRA 1.0 mg/kg + DEX at 50 µg, ATO at 0.75 mg/kg, or ATRA + ATO every two days. At day 14, blood samples were collected from the heart and analysed for total numbers of NB4 WT and TG2-KO cells by FACS and human-ALU-based RT-qPCR analyses. Graphs show the mean ± SD values after 14 days ($n = 4$). Statistical analysis was conducted by two-way ANOVA (Bonferroni post hoc test; *$p < 0.05$, **$p < 0.01$ and ***$p < 0.001$, ****$p < 0.0001$). **B** Representative western blot showing expression of TG2, p-AKT (S473, T308), AKT, p-mTOR (2481, 2448), mTOR, pro-caspase3/truncated forms, and GAPDH proteins in the total cell lysate or in a cell population sorted by Annexin-V labelling ($n = 7$). **C** Representative IP-western blot showing plasma membrane CD18 and TG2 protein expression levels following ATRA treatment of NB4 WT cells ($n = 5$). **D** Representative co-immunoprecipitation-Western-blot showing plasma membrane and total cell lysate TG2, CD18, SRC, p-mTOR (2481, 2448), p-AKT (S473, T308), p85, p-p85, p110, PTEN, and p-PTEN protein expression levels in NB4 WT cells following upon ATRA, ATRA + NC9 (30 µM), or ATRA + PP2 (20 µM) treatment ($n = 3$). **E** TG2-dependent signalosome formation and its inhibition by NC9 or PP2. **F** Interaction map of the bait and prey proteins in plasma membrane fractions of differentiated NB4 WT cells detected by modified far western blot (black dots) and by LC-MS/MS method (orange dots). Representative co-immunoprecipitation-western-blot showing plasma membrane containing TG2, mTOR, p-mTOR (2481, 2448), AKT, p-AKT (S473, T308), p85, p110, PTEN, CD18, SRC protein expression levels in NB4 WT cells following upon ATRA treatment for 5 days ($n = 3$). **G** Interaction map of the bait and prey proteins in plasma membrane fractions of differentiated NB4 WT CD18$^{-/-}$ cells detected by modified far western blot. The left panel's representative western blots show the expression of the detected prey proteins with TG2 antibody in the absence of CD18. In contrast, the right panel's western blot result shows the same PVDF membrane, developed with CD18 antibody ($n = 3$).

4C). Our examination of TG2 in Annexin-V negative, living and Annexin-V positive, apoptotic cells showed that the amount of TG2 is below the detection limit in Annexin-V-positive, apoptotic cells but is measurable in Annexin-V-negative cells (Fig. 5B 2nd and 3rd panels).

TG2 in its GTP-bound/closed/signalling-active form may act as an organisational constituent or a signalosome for PI3K-AKT-mTOR-FOXO3 signal transduction by promoting the assembly of multiprotein signal transduction complexes at the plasma membrane. Formation of this signalosome is a time-dependent process, where the enrichment of the TG2 is crucial (Supplementary Fig. 6). This enables the establishment of false spatially concentrated and site-specific signals with atypically increased PI3K, phospho-mTOR S2481, and phospho-AKT S473 signalling activities. Both the specificity and the regulation of signal transduction are extraordinarily increased, since certain signalling proteins, such as CD18, c-SRC, phospho-AKT T308, S473, phospho-mTOR S2481 and S2448, can associate with the GTP-bound/ closed/signalling-active TG2. The open/transamidase-active conformation is locked by NC9, a TG2-selective irreversible inhibitor, thereby terminating GTP binding and the TG2 signalosome. Treatment with PP2, an inhibitor of SRC, can also accomplish this.

The TG2 polypeptide chain is composed of 687 amino acids and four distinct protein domains. Conformational states of TG2 are primarily regulated by nucleotides and Ca^{2+}, two major regulators that have a significant impact on the conformational states of TG2. Upon Ca^{2+} binding, TG2 undergoes a nearly 120 angstroms intramolecular shift, which exposes or hides functional surfaces that can react with transitory or permanent interaction partners. Most of TG2's identified protein-protein interactions (PPI) are mediated by short linear motifs (SLiMs, 3–20 amino acids) that commonly overlap with one of its 13 intrinsically disordered regions (IDRs), demonstrated by Kanchan et al. 2013 [23]. Multiple IDRs and several short linear motifs in close proximity to or at the intrinsically disordered regions point to the presence of an interacting network around TG2 that is not constant over the timespan of days, but rather intermittently makes contact with regulatory partners. Thus, in a limited number of timepoints only select interactions will be detected simultaneously. Perhaps, in this case, at day 2, we can observe such a protein-protein interaction where the interaction of TG2 and CD18 is energetically more favoured than with another PPI proteins (Supplementary Fig. 6).

More practically, it is possible to conclude that the "signalosome" assembly is a time-dependent mechanism. At day 2 of the
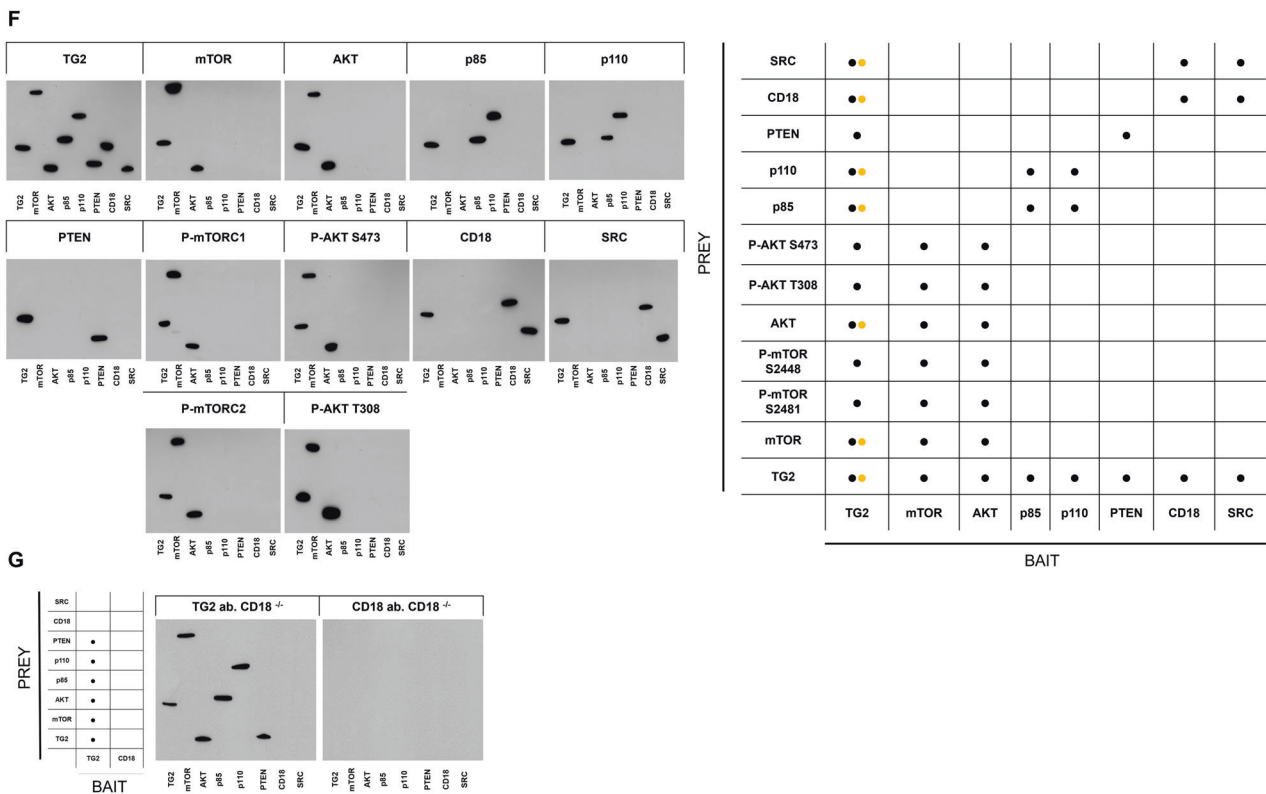
Fig. 5 (Continued)

ATRA-induced differentiation process, we could see that the "upstream" (CD18, SRC) and "downstream" (mTOR, AKT, P85, P110, PTEN) components were bound to TG2. It is important to note that this does not imply that the complex has yet to be formed; TG2 could bind to these components independently of the formation of the signalosome. However, given that CD18 resin was able to pull down TG2, whereas CD18 resin was able to pull down the TG2 in the co-immunoprecipitation experiments, this could imply that the signalosome formation at the start of differentiation could only assemble the "upper" part of the complex, with the lower proteins attaching to the complex later on. These findings suggest that signalosome formation is a time-dependent process involving the TG2 "scaffold" mechanism.

The formation of "signalosomes," multimolecular protein complexes composed of distinct combinations of signalling pathway proteins directed into different intracellular compartments via their association with adaptor or scaffold proteins, can contribute to signalling compartmentalisation. Scaffold proteins mediate the branching of signalling information to several outputs that become part of the assembled complex. Co-localisation of pathway components normally allows for both efficient signal transmission between adjacent molecules and the prevention of undesirable crosstalk with other pathways in the cells. A large number of distinct signalling components, all of which may be involved in multiple signalling pathways, regulate various cellular processes both temporally and spatially. Many abnormally regulated signalling pathways have been found in cancer cells. Additionally, specific protein-protein interactions are prerequisites for the uncontrolled activation or inhibition of these signalling pathways. The AKT kinase, for example, binds to numerous proteins in the PI3K/AKT signalling pathway, but the fully phosphorylated AKT binds to more than 100 proteins, including the Bcl-2-associated death promoter (BAD), caspase-9, mTORC, various forkhead box protein O (FOXO) proteins, mouse double minute 2 homologue (MDM2), glycogen synthase kinase 3 (GSK3),

and tuberous sclerosis 1 (TSC1) [24]. AKT has been shown to bind to the IκB kinases, IKKα and IKKβ, in the NF-κB signalling pathway. AKT phosphorylates IKKα on threonine (Thr23), activating the NF-κB signalling pathway, which causes immune and inflammatory responses. Since IKKβ is an AKT direct target, the cell survival, and anti-apoptotic functions of NF-κB signalling are intrinsically linked to AKT/IKKβ signalling activation [25–27]. According to our previous findings, NC9-induced conformational changes in TG2 have a significant impact on the NF-κB signalling pathway. In the presence of NC9, the ATRA-induced total amount of TG2 protein is reduced, along with the nuclear translocation of TG2, resulting in a significant increase in cytosolic TG2. A decrease in nuclear TG2 is associated with lower total levels of nuclear p50, p65/RelA, and phospho-p65/RelA proteins in NB4 WT cells. The transcriptionally active form of phospho-p65, on the other hand, is significantly elevated in the cytosol. This suggests that TG2 can easily translocate and help p65/RelA in its GTP-bound closed conformation into the nucleus. When TG2 loses its ability to adopt its GTP-bound closed conformation due to NC9 modification, the cytosolic accumulation of both TG2 and p65/RelA results in low NF-κB transcription activity and, as a result, significantly reduced production of inflammatory cytokines and chemokines [12]. Research on the protein-protein interaction between TG2 and RelA is now under way. These current and previous results suggest that the GTP-bound closed conformation of TG2 favours the formation of protein-protein interactions that mediate the branching of pathways to multiple outputs, in this case the CD18/SRC/TG2/PI3K/PTEN/AKT/mTOR pathways.

In summary, the atypical expression of GTP-bound TG2 is an upstream signal activating a signalosome platform that hyper-activates a PI3K, phospho-AKT S473, and phospho-mTOR S2481 signalling axis via CD18, along with a robust PTEN inactivation, to maintain phospho-FOXO3 in a transcriptionally inactive state and promote cell survival. TG2 is dysregulated in many tumours; therefore, reducing TG2 levels and/or modifying

the open/transamidase-active form may represent promising strategies to sensitise tumour cells to cancer therapy.

REFERENCES
1. Eckert RL, Fisher ML, Grun D, Adhikary G, Xu W, Kerr C. Transglutaminase is a tumor cell and cancer stem cell survival factor. Mol Carcinog. 2015;54:947–58.
2. Chen F, Zhang Y, Varambally S, Creighton CJ. Molecular correlates of metastasis by systematic pan-cancer analysis across the Cancer Genome Atlas. Mol Cancer Res. 2019;17:476–87.
3. Tabolacci C, De Martino A, Mischiati C, Feriotto G, Beninati S. The role of tissue transglutaminase in cancer cell initiation, survival and progression. Med Sci. 2019;7:19.
4. Benedetti L, Grignani F, Scicchitano BM, Jetten AM, Diverio D, Lo Coco F, et al. Retinoid-induced differentiation of acute promyelocytic leukemia involves PML-RARalpha-mediated increase of type II transglutaminase. Blood. 1996;87:1939–50.
5. Balajthy Z, Csomós K, Vámosi G, Szántó A, Lanotte M, Fésüs L. Tissue-transglutaminase contributes to neutrophil granulocyte differentiation and functions. Blood. 2006;108:2045–54.
6. Sanz MA, Lo-Coco F. Modern approaches to treating acute promyelocytic leukemia. J Clin Oncol. 2011;29:495–503.
7. Sanz MA, Montesinos P. How we prevent and treat differentiation syndrome in patients with acute promyelocytic leukemia. Blood. 2014;123:2777–82.
8. de Thé H, Pandolfi PP, Chen Z. Acute promyelocytic leukemia: a paradigm for oncoprotein-targeted cure. Cancer Cell. 2017;32:552–60.
9. Zhu H-H, Hu J, Lo-Coco F, Jin J. The simpler, the better: oral arsenic for acute promyelocytic leukemia. Blood. 2019;134:597–605.
10. Cicconi L, Platzbecker U, Avvisati G, Paoloni F, Thiede C, Vignetti M, et al. Long-term results of all-trans retinoic acid and arsenic trioxide in non-high-risk acute promyelocytic leukemia: update of the APL0406 Italian-German randomized trial. Leukemia. 2020;34:914–8.
11. Csomós K, Német I, Fésüs L, Balajthy Z. Tissue transglutaminase contributes to the all-trans-retinoic acid–induced differentiation syndrome phenotype in the NB4 model of acute promyelocytic leukemia. Blood. 2010;116:3933–43.
12. Jambrovics K, Uray IP, Keresztessy Z, Keillor JW, Fésüs L, Balajthy Z. Transglutaminase 2 programs differentiating acute promyelocytic leukemia cells in all-trans retinoic acid treatment to inflammatory stage through NF-κB activation. Haematologica. 2019;104:505–15.
13. Mirabilii S, Ricciardi MR, Piedimonte M, Gianfelici V, Bianchi MP, Tafuri A. Biological aspects of mTOR in leukemia. Int J Mol Sci. 2018;19:2396.
14. Liu P, Gan W, Chin YR, Ogura K, Guo J, Zhang J, et al. PtdIns (3, 4, 5) P3-dependent activation of the mTORC2 kinase complex. Cancer Discov. 2015;5:1194–209.
15. Sarbassov DD, Guertin DA, Ali SM, Sabatini DM. Phosphorylation and regulation of Akt/PKB by the rictor-mTOR complex. Science 2005;307:1098–101.
16. Eijkelenboom A, Burgering BM. FOXOs: signalling integrators for homeostasis maintenance. Nat Rev Mol Cell Biol. 2013;14:83–97.
17. Zhang X, Tang N, Hadden TJ, Rishi AK. Akt, FoxO and regulation of apoptosis. Biochim Biophys Acta Mol Cell Res. 2011;1813:1978–86.
18. Liu Y, Ao X, Ding W, Ponnusamy M, Wu W, Hao X, et al. Critical role of FOXO3a in carcinogenesis. Mol Cancer. 2018;17:1–12.
19. Funakoshi K, Bagheri M, Zhou M, Suzuki R, Abe H, Akashi H. Highly sensitive and specific Alu-based quantification of human cells among rodent cells. Sci Rep. 2017;7:1–12.
20. Sato Y, Kameya M, Arai H, Ishii M, Igarashi Y. Detecting weak protein-protein interactions by modified far-western blotting. J Biosci Bioeng. 2011;112:304–7.
21. Wu Y, Li Q, Chen XZ. Detecting protein-protein interactions by Far western blotting. Nat Protoc. 2007;2:3278–84.
22. Kim YE, Kim KE, Kim KK. In Vivo Crosslinking of Histone and RNA-Binding Proteins. In: RNA-Chromatin Interactions, New York, NY: Humana; 2020, pp. 75–88.
23. Kajal K, Elvan E, Robert K, Zsófia S, Mónika F, László F. Identification of a specific one amino acid change in recombinant human transglutaminase 2 that regulates its activity and calcium sensitivity. Biochem J. 2013;455:261–72.
24. Manning BD, Cantley LC. AKT/PKB signaling: navigating downstream. Cell. 2007;129:1261–74.
25. Ozes ON, Mayo LD, Gustin JA, Pfeffer SR, Pfeffer LM, Donner DB. NF-kappaB activation by tumour necrosis factor requires the Akt serine-threonine kinase. Nature. 1999;401:82–85.
26. Lu Y, Wahl LM. Production of matrix metalloproteinase-9 by activated human monocytes involves a phosphatidylinositol-3 kinase/Akt/IKKα/NF-κB pathway. J Leukoc Biol. 2005;78:259–65.
27. Kerr C, Szmacinski H, Fisher ML, Nance B, Lakowicz JR, Akbar A, et al. Transamidase site-targeted agents alter the conformation of the transglutaminase cancer stem cell survival protein to reduce GTP binding activity and cancer stem cell survival. Oncogene. 2017;36:2981–2990.

AUTHOR CONTRIBUTIONS
ZB designed the study and conducted some experiments, KJ performed most of the experiments, PB, KJ and IS performed the flow cytometry analyses, AP, ZS, ZK and ZC contributed to the mice experiments; Writing - Original Draft, BZ and KJ, Writing – Review and Editing, IPU, BZ, KJ and LF. Funding acquisition, LF, ZB, and IPU.

COMPETING INTERESTS
The authors declare no competing interests.

ADDITIONAL INFORMATION
Supplementary information The online version contains supplementary material available at https://doi.org/10.1038/s41419-023-05748-6.

Correspondence and requests for materials should be addressed to Zoltán. Balajthy.

Reprints and permission information is available at http://www.nature.com/reprints

Publisher's note Springer Nature remains neutral with regard to jurisdictional claims in published maps and institutional affiliations.